Neurotoxicology 71 (2019) 138–149

Contents lists available at ScienceDirect

Neurotoxicology

journal homepage: www.elsevier.com/locate/neuro

Blockade of GluN2B-containing NMDA receptors reduces short-term brain damage induced by early-life status epilepticus

Cássio Morais Loss[a,b,*,1], Natã Sehn da Rosa[a,1], Régis Gemerasca Mestriner[c], Léder Leal Xavier[d], Diogo Losch Oliveira[a]

[a] Cellular Neurochemistry Laboratory, Departamento de Bioquímica, Instituto de Ciências Básicas da Saúde, Universidade Federal do Rio Grande do Sul, Porto Alegre, Rio Grande do Sul, Brazil
[b] Cellular Biochemistry Laboratory, Departamento de Bioquímica, Instituto de Ciências Básicas da Saúde, Universidade Federal do Rio Grande do Sul, Porto Alegre, Rio Grande do Sul, Brazil
[c] Neurorehabilitation and Neural Repair Research Group, Pontifícia Universidade Católica do Rio Grande do Sul, Porto Alegre, Rio Grande do Sul, Brazil
[d] Laboratory of Cell and Tissue Biology, School of Sciences, Pontifícia Universidade Católica do Rio Grande do Sul, Porto Alegre, Rio Grande do Sul, Brazil

ARTICLE INFO

Keywords:
Epilepsy
CI-1041
CP-101606
Neuroinflammation
Development
Neurodegeneration

ABSTRACT

Status epilepticus (SE) during developmental periods can cause short- and long-term consequences to the brain. Brain damage induced by SE is associated to NMDA receptors (NMDAR)-mediated excitotoxicity. This study aimed to investigate whether blockade of GluN2B-containing NMDAR is neuroprotective against SE-induced neurodegeneration and neuroinflammation in young rats. Forty-eight Wistar rats (16 days of life) were injected with pilocarpine (60 mg/kg; i.p.) 12–18 h after LiCl (3 mEq/kg; i.p.). Fifteen minutes after pilocarpine administration, animals received i.p. injections of saline solution (0.9% NaCl; SE + SAL group), ketamine (a non-selective and noncompetitive NMDAR antagonist; 25 mg/kg; SE + KET), CI-1041 (a GluN2B-containing NMDAR antagonist; 10 mg/kg; SE + CI group) or CP-101,606 (a NMDAR antagonist with great selectivity for NMDAR composed by GluN1/GluN2B diheteromers; 10 mg/kg; SE + CP group). Seven days after SE, brains were removed for Fluoro-Jade C staining and Iba1/ED1 immunolabeling. GluN2B-containing NMDAR blockade by CI-1041 or CP-101,606 did not terminate LiCl-pilocarpine-induced seizures. SE + SAL group presented intense neurodegeneration and $Iba1^+/ED1^+$ double-labeling in hippocampus (CA1 and dentate gyrus; DG) and amygdala (MePV nucleus). Administration of CP-101,606 did not alter this pattern. However, GluN2B-containing NMDAR blockade by CI-1041 reduced neurodegeneration and $Iba1^+/ED1^+$ double-labeling in hippocampus and amygdala similar to the reduction observed for SE + KET group. Our results indicate that GluN2B-containing NMDAR are involved in SE-induced neurodegeneration and microglial recruitment and activation, and suggest that stopping epileptic activity is not a condition required to prevent short-term brain damage in young animals.

1. Introduction

Status epilepticus (SE) is defined as a condition of abnormally self-sustained prolonged seizures (Trinka et al., 2015). This life-threatening neurological disorder presents higher incidence during infancy and childhood (Gross-Tsur and Shinnar, 1993; Holmes, 1997) wherein several studies have reported short- and long-term consequences to the developing brain. These consequences include neuronal cell death, microglial recruitment and activation, and abnormal neuronal network formation (de Oliveira et al., 2008; Fujikawa, 1995; Jakubs et al., 2006; Kubova et al., 2004; Loss et al., 2012; Mishra et al., 2015; Rice et al., 1998; Sankar et al., 1998; Yankam Njiwa et al., 2016). Neuronal cell death caused by SE has been frequently associated to an excessive activation of NMDA receptors (NMDAR) (Holopainen, 2008) and some studies have demonstrated that administration of NMDAR antagonists was neuroprotective against SE-induced neurodegeneration in both pre- and post-SE onset treatment regimens (Clifford et al., 1990; Fujikawa, 1995; Holmes, 2004; Loss et al., 2012).

Functional NMDAR, which are heterotetrameric complexes composed by the obligatory GluN1 subunits and a combination of GluN2 and/or GluN3 subunits (Di Maio et al., 2011), are found both inside and outside the synapse (synaptic and extrasynaptic NMDAR, respectively).

* Corresponding author at: Departamento de Bioquímica, ICBS, UFRGS, Rua Ramiro Barcelos 2600-Anexo, 90035-003, Porto Alegre, Rio Grande do Sul, Brazil.
E-mail address: cassio.m.loss@gmail.com (C.M. Loss).
[1] These authors contributed equally to data collection, data analysis and interpretation, and drafting the article.

https://doi.org/10.1016/j.neuro.2019.01.002
Received 22 June 2018; Received in revised form 22 November 2018; Accepted 9 January 2019
Available online 11 January 2019
0161-813X/

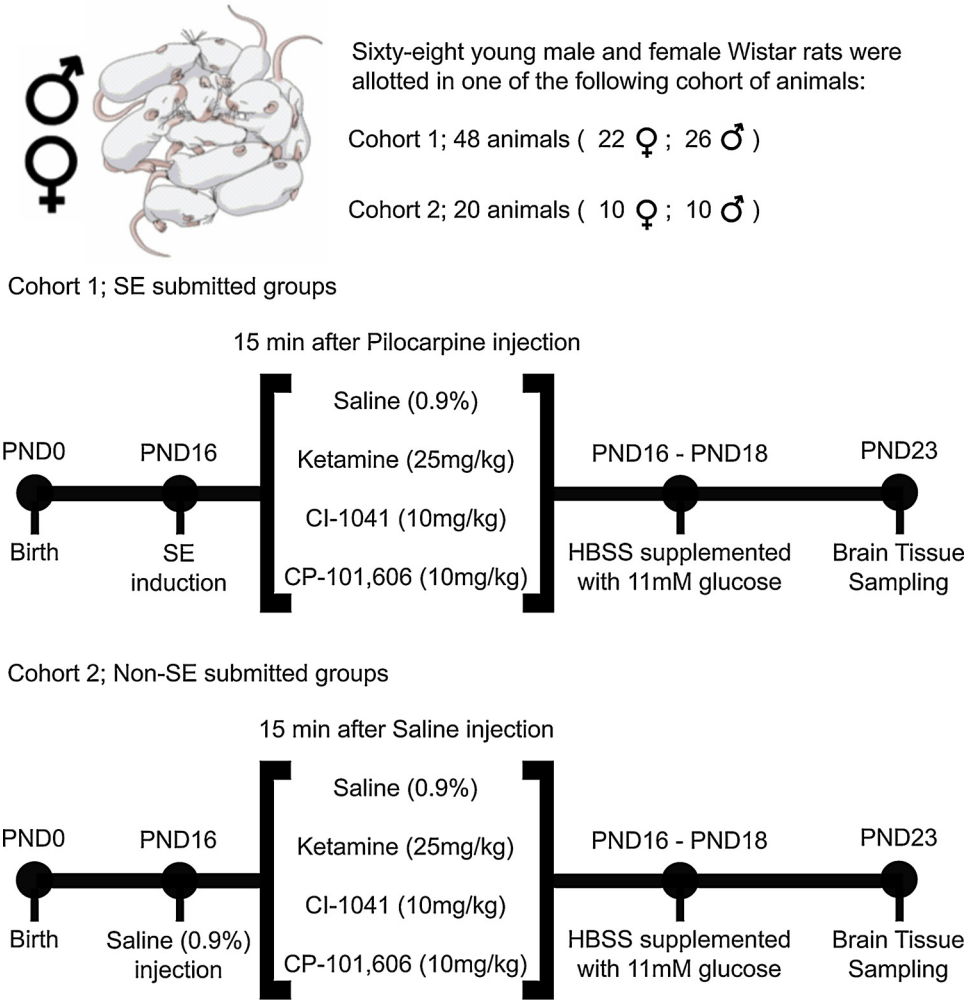

Fig. 1. Experimental design. Pups from both sexes and from several litters were used in this study. They were subjected to one of two independent experiments. The first cohort of animals (48 pups) was subjected to LiCl-pilocarpine-induced SE and 15 min after pilocarpine injection were assigned to one of the following treatments: (i) saline (0.9%); (ii) ketamine (25 mg/kg); (iii) CI-1041 (10 mg/kg); or (iv) CP-101,606 (10 mg/kg). Especial care procedure (injection of HBSS supplemented with 11 mM glucose during three days) was adopted to prevent high mortality rate. Seven days after SE onset, animals had their brains collected to histological analysis. The second cohort of animals (20 pups) was handled exactly the same way as the first cohort of animals, except that they received saline (0.9%) instead of pilocarpine.

These different localizations of the NMDAR reflect different subtypes of the receptor, being that synaptic NMDAR are predominantly GluN1/GluN2A diheteromers and GluN1/GluN2A/GluN2B triheteromers, whereas extrasynaptic NMDAR are enriched in GluN2B subunit (mostly GluN1/GluN2B diheteromers) (Gladding and Raymond, 2011; Hardingham and Bading, 2010; Hardingham et al., 2002).

Activation of NMDAR under physiological conditions contribute to modulation of several intracellular signaling pathways *via* Ca^{+2} influx, which occurs through a ionic pore located inside the receptor complex (Di Maio et al., 2011). However, during excessive activation of NMDAR, such as that observed in SE, the cytosolic free Ca^{+2} concentration increases quickly and leads neurons to death (Olney, 2003). Previous studies have suggested that extrasynaptic NMDAR (*i.e.*, GluN2B-enriched receptors) are the NMDAR subpopulation responsible for this Ca^{+2} influx and subsequent neuronal death (Hardingham and Bading, 2010; Hardingham et al., 2002).

Upon sensing pathological signals, including seizures and SE-induced neurodegeneration, microglial cells (the resident immune cells of the brain) become reactive and promptly undergo biochemical changes producing pro-inflammatory cytokines, which leads to a self-sustained cycle of microglial recruitment and activation (Liu et al., 2017; Schartz et al., 2016; Wyatt-Johnson et al., 2017). This neuroinflammatory scenario has been suggested as a key event in epileptogenesis (Bertoglio et al., 2017; Choi and Koh, 2008; Liu et al., 2017; Schartz et al., 2016; Vezzani et al., 2011).

In the present study we investigated whether blockade of GluN2B-containing NMDAR is sufficient to prevent neuronal cell death and microglial recruitment and activation induced by early-life SE. We hypothesized that excessive activation of extrasynaptic NMDAR is a key mechanism implicated in SE-induced neurodegeneration. We expected that GluN2B-containing NMDAR blockade by specific antagonist could reduce neuronal loss and, consequently, neuroinflammation (measured by microglial recruitment and activation).

2. Experimental procedure

2.1. Materials

Pilocarpine hydrochloride was purchased from Sigma-Aldrich (USA). CP-101,606 (a NMDAR antagonist with great selectivity for GluN1/GluN2B diheteromers (Chazot et al., 2002; Hansen et al., 2014)) and CI-1041 (a GluN2B-containing NMDAR antagonist (Chen et al., 2003; Nagy et al., 2004)) were kindly donated by Pfizer Inc., Ann Arbor (MI, USA). Fluoro-Jade C was purchased from Chemicon, Inc. (USA). Other chemicals were purchased from Nuclear (Brazil). All solutions were prepared so that the injection volume was 5 mL/kg.

2.2. Subjects

Sixty-eight young male and female Wistar rats (15 postnatal days – PND15) were obtained from breeding colony of the Department of Biochemistry of Universidade Federal do Rio Grande do Sul. Birth was defined as postnatal day 0 (PND0). Animals were housed in standard polypropylene cages with food and water *ad libitum,* under a 12 h controlled light/dark photoperiod cycle (lights on at 7:00 am) with room temperature adjusted to 21 ± 2 °C. All procedures were

conducted according to the Guide for Care and Use of Laboratory Animals from National Institutes of Health (NIH Publications No. 8023, revised 1978), the Brazilian Law for Care and Use of Laboratory Animals (Law 11794/2008), and were previously approved by the Ethics Committee from Universidade Federal do Rio Grande do Sul (protocol number #21369).

2.3. Induction of status epilepticus

Forty-eight rat pups (from both sexes) were injected with a solution of LiCl (127.2 mg/kg i.p.) 12–18 h prior to pilocarpine (60 mg/kg i.p.) administration on PND16 (de Oliveira et al., 2008) (Fig. 1). Immediately after pilocarpine injection, rats were put in individual plastic cages at 34 °C (nest temperature) during 1.5 h for observation of seizures which were evaluated only by behavioral measures. Fifteen min after pilocarpine administration, pups received i.p. injections of vehicle (0.9% NaCl; SE + SAL group), or ketamine (25 mg/kg (Loss et al., 2012); SE + KET), or CP-101,606 (10 mg/kg (Brackett et al., 2000); SE + CP group) or CI-1041 (10 mg/kg (Kovacs et al., 2004; Ouattara et al., 2009); SE + CI group). Animals were pseudo-randomly assigned to their respective experimental groups in order to obtain a similar ratio between males and females within each experimental group (about 50% of each sex). Each experimental group contained pups from several litters to minimize litter-specific effects. Rats were allowed to spontaneously recover from SE. In order to prevent high mortality rates, pups received i.p. injections of HBSS supplemented with 11 mM glucose 1.5, 4, 7, 24, 36, 48 and 60 h after pilocarpine injection. The body weight was assessed daily until the last experimental day. Seven days after SE induction, animals were used to determine SE-induced neuronal loss (Fluoro-Jade C staining) and microglial recruitment and activation (Iba1/ED1 double-labeling immunofluorescence). This time-point was chosen because we wanted to assess brain damage in a period in which both neuronal degeneration and microglial recruitment and activation were elevated (Ekdahl et al., 2003; Jakubs et al., 2006; Liu et al., 2017; Schartz et al., 2016; Wang et al., 2008; Wyatt-Johnson et al., 2017; Yankam Njiwa et al., 2016).

In order to verify if NMDAR antagonist's treatment could induce neurodegeneration *per se*, another cohort of 20 animals (from both sexes) was treated with LiCl-saline (Non-SE submitted groups) followed by injection of NMDAR antagonists (at same doses described above) (Fig. 1). After, animals were housed and handled as the same manner of SE-induced animals (N = 5 animals per group).

2.4. Brain tissue sampling

Seven days after SE induction rats were deeply anesthetized i.p. with ketamine (90 mg/kg) and xylazine (12 mg/kg) and sequentially perfused through the heart with 100 mL of 0.1 M sodium phosphate buffer, pH 7.4, followed by 100 mL of 4% paraformaldehyde in 0.1 M sodium phosphate buffer, pH 7.4. Brains were removed and immersed for 4 h in the same fixative solution. After post-fixation, samples were transferred to a 15% followed by transfer to 30% sucrose until the brains sank to the bottom of the chamber. Coronal slices (50 µm) on representative microscopic fields, were obtained using a Leica CM1850 Cryostat, approx. Bregma: -2.56 mm; Interaural: 6.44 mm until Bregma: −3.80 mm; Interaural: 5.20 mm, corresponding to figures 30–35 of Paxinos and Watson atlas (1998).

2.4.1. Fluoro-Jade C staining

Fluoro-Jade C (FJC) staining was based on Schmued et al. (2005). Coronal slices were mounted onto gelatin-coated slides and dried at room temperature overnight. Slides were immersed twice in xylene for 10 min followed by absolute ethanol for 3 min. Then, slides were rinsed for 2 min in 70% ethanol, 2 min in distilled water, and incubated in 0.06% potassium permanganate solution for 10 min. Slides were rinsed in distilled water for 2 min and transferred for 10 min to a 0.0001% FJC solution dissolved in 0.1% acetic acid, washed three times for 1 min with distilled water, dried at room temperature overnight, dehydrated in xylene for 2 min, and then cover-slipped with DPX. Sections corresponding to hippocampal subfields CA1 and Dentate Gyrus (DG), and amygdala (medial amygdaloid nucleus - MePV) were digitalized using a Zeiss Axio Imager A1 microscopy. Due to the large extent of CA1 and DG hippocampal subfields, the entire region was brief scanned before digitalization. Once neurodegeneration was anisotropic among sections in these regions, a single digitalization per section was performed after the identification of the most damaged portion of the region (*i.e.*, portion of the region which presented the greatest number of FJC^+ cells). By employing this procedure we increased isotropy of the damage among sections, reducing data variability and minimizing underestimation of neurodegeneration induced by SE. Estimation of FJC^+ neuronal density (number of FJC^+ neurons/mm^2) was performed using Image-Pro Plus Version 6.0 software (Media Cybernetics Inc., USA). Briefly, starting in a random point in images obtained from CA1 and DG, three equidistant areas of interest (AOIs) with square shape, measuring 1500 μm^2 were overlaid in each image. For MePV nucleus, starting in a random point, five equidistant AOIs with square shape and measuring 3300 μm^2 were overlaid in each image. AOIs were designed to allow the investigator to count at most 10 cells per AOI to minimize any errors in counting. FJC^+ neurons located inside this square or intersected by the upper and/or right edges of the square were counted, while FJC^+ neurons intersected by the lower and/or left edges of the square were not counted. Cells (neuronal somas) exhibiting bright green fluorescence were counted while FJC^+ fragments were not counted. At least five slices per region were analyzed per animal. The investigator who analyzed the images was blinded to the analysis (de Senna et al., 2017; Mestriner et al., 2015; Saur et al., 2014).

2.4.2. Iba1/ED1 double-labeling immunofluorescence

For Iba1/ED1 double-labeling (Wu et al., 2005), free-floating sections were washed 3 times with 0.1 M PBS and then permeabilized with TPBS (0.3% Triton X-100 in 0.1 M PBS) for 1 h. To quench endogenous peroxidase activity, sections were incubated in solution containing 2% H_2O_2 in 0.1 M PBS for 30 min. After washing with 0.1 M PBS for 5 min, sections were incubated in blocking solution (1% Albumin in TPBS) for 1 h followed by incubation in mouse-anti-ED1 (1:200, Serotec Ltd., Oxford, UK) and rabbit-anti-Iba1 (1:1000, Wako Chemicals, Neuss, Germany) for 24 h at 4 °C. After washing 3 times with 0.1 M PBS, they were incubated for 2 h in Alexa Fluor goat anti-rabbit 488 and Alexa Fluor goat anti-mouse 555 secondary antibodies (1:1000, Molecular Probes, Oregon, USA) at room temperature in dark. Sections were washed 3 times with 0.1 M PBS, mounted onto gelatin-coated slides and cover-slipped with Fluoromount. Images were digitalized using a Leica SP8 confocal microscope. Due to the large extent of CA1 and DG hippocampal subfields, the entire region was brief scanned before digitalization. Once microgliosis (*i.e.*, prominent microglial activity represented by increased Iba1 and ED1 immunoreactivity) was anisotropic among sections in these regions, a single digitalization per section was performed after the identification of the most damaged portion of the region (*i.e.*, the portion of the region which presented the greatest number of $Iba1^+/ED1^+$ double-staining cells). By employing this procedure we increased isotropy of the damage among sections, reducing data variability and minimizing underestimation of microgliosis induced by SE. The estimation of $Iba1^+$ and $ED1^+$ cells densities (number of $Iba1^+$ and $ED1^+$ cells/mm^3) was obtained using an adaptation of optical disector. Briefly, a square counting frame with 844 μm^2 was randomly overlaid onto the region analyzed and $Iba1^+$ and $ED1^+$ cells were counted at different focal planes in the z axis throughout the brain slice. The disector's height ranged from 10 to 20 µm. Thus, the disector's volume ranged from 8.440 to 16.880μm^3. Disector's were designed to allow the investigator to count at most 10 cells per disector to minimize any errors in counting. The $Iba1^+$ and $ED1^+$ cells inside this square overlaying the "including" borders (upper and right) were

counted, and Iba1$^+$ and ED1$^+$ cells overlaying the "excluding" borders (lower and left) were not counted. At least five slices per region were analyzed per animal. The investigator who analyzed the images was blinded to the analysis (Costa-Ferro et al., 2010; Dall'Oglio et al., 2013).

2.5. Statistical analysis

All data were analyzed using both sexes combined. Data of mortality rate were analyzed by Mantel–Cox test. The daily variation of body weight was calculated as the difference between the body mass in one day and the body mass in the previous day. Data of body weight are expressed as mean ± SD and were analyzed by two-way ANOVA with repeated measures (where appropriated, Holm-Sidak's post hoc test for multiple comparisons was used to compare the mean of each group with the mean of SE + SAL group). Histological data which passed in Brown-Forsythe test are expressed as mean ± SD and were analyzed by one-way ANOVA (where appropriated, Holm-Sidak's post hoc test for multiple comparisons was used to compare the mean of each group with the mean of SE + SAL group). Histological data which did not pass in Brown-Forsythe test are expressed as median and the interquartile ranges and were analyzed by Kruskal-Wallis test (where appropriated, Dunn's post hoc test for multiple comparisons was used to compare the mean rank of each group with the mean rank of SE + SAL group). $P < 0.05$ was considered statistically significant.

3. Results

3.1. Effect of GluN2B-containing NMDAR blockade on convulsive pattern of SE

The behavioral convulsive pattern of LiCl-pilocarpine-treated animals was similar to those described by de Oliveira et al. (2008) and Loss et al. (2012). Systemic administration of LiCl-pilocarpine produced defecation, salivation, body tremor, and scratching within 2–8 min. This behavioral pattern progressed to increased levels of motor activity and culminated in SE in all animals within 8–13 min. SE was characterized by sustained orofacial automatisms, salivation, chewing, forelimb clonus, loss of righting reflex and falling (equivalent to stage 5 of Racine's scale).

As already described (Loss et al., 2012), treatment with ketamine (SE + KET group) 15 min after pilocarpine administration reduced the intensity of sustained orofacial automatisms, forelimbs clonus and chewing, without recovering the loss of righting reflex. However, GluN2B-containing NMDAR blockade by CI-1041 (SE + CI group) or CP-101,606 (SE + CP group) 15 min after pilocarpine administration (*i.e.*, after SE onset) did not affect the behavioral pattern of SE when compared with animals from SE + SAL group. Administration of CI-1041 or CP-101,606 did not induce any behavioral alteration in Non-SE submitted animals.

3.2. Effect of GluN2B-containing NMDAR blockade on mortality rate of SE-induced animals

Fifty percent of animals from SE + SAL group (6 of 12) died up to 24 h after pilocarpine injection. Administration of GluN2B-containing NMDAR antagonists did not alter this mortality rate (5 of 11 for CI-1041, *i.e.*, 45%; 8 of 16 for CP-101,606, *i.e.*, 50%, being 7 up to 24 h after SE onset and 1 at PND19). Only 1 of 9 animals (11%) which received ketamine after SE onset died (Fig. 2a). However, no statistical differences between groups were found (Chi-square = 4.12; $P = 0.25$). Administration of ketamine, CI-1041 or CP-101,606 in animals that were not injected with pilocarpine (Non-SE animals) did not cause death (data not shown).

3.3. Effect of GluN2B-containing NMDAR blockade on weight gain after SE

Two-way ANOVA with repeated measures revealed a significant interaction between time and treatment [$F(21,168) = 2.03$; $P = 0.0074$] and a significant effect of time on weight gain of animals [$F(7,168) = 138.9$; $P < 0.0001$] (Fig. 2b). All groups presented a significant weight loss in the first day after SE induction ($\Delta 16,17 = -4.8 \pm 0.6$ for SE + SAL; -4.8 ± 0.3 for SE + KET; -4.2 ± 0.2 for SE + CP; and -6.5 ± 0.4 for SE + CI; $F = 7.0$; $P < 0.0001$). Animals from SE + KET and SE + CI groups presented with faster weight recovery as they started to gain weight in PND18 while SE + SAL group only started to gain weight in PND20 (Fig. 2b). Animals from SE + CP group presented a weight gain profile similar to SE + SAL group (Fig. 2b and c). A representation of cumulative weight gain profile is depicted in Fig. 2c.

3.4. Effect of GluN2B-containing NMDAR blockade on SE-induced neurodegeneration

The FJC$^+$ staining cells showed a bright green color in the somas and fine processes with neuronal profiles (dendrites, axons and axon terminals) (Schmued et al., 2005; Wang et al., 2008). Seven days after SE onset, it was observed that LiCl-pilocarpine administration induced massive neurodegeneration (indicated by increased FJC staining) in several brain regions, including CA1, DG, and amygdala (medial amygdaloid nucleus - MePV) (Fig. 3). Administration of CP-101,606 after SE onset did not alter the number of FJC$^+$ neurons in comparison to SE + SAL group in all analyzed regions. However, animals from both SE + KET and SE + CI groups presented a reduced number of FJC$^+$neurons in DG [$KW(4,26) = 17.55$; $P = 0.0005$] and MePV [$KW(4,25) = 18.83$; $P = 0.0003$]. Moreover, a reduction in the number of FJC$^+$ neurons was observed in CA1 hipocampal subfield for SE + KET group when compared to SE + SAL group [$KW(4,26) = 14.28$; $P = 0.0026$] (Fig. 3). FJC$^+$ neurons were not observed in the brain of Non-SE animals (data not shown).

3.5. Effect of GluN2B-containing NMDAR blockade on SE-induced microglial recruitment and activation

An intense Iba1$^+$/ED1$^+$ double-labeling (indicated by high fluorescence and brightness) was observed in several brain regions seven days after SE onset. Ramified (resting) and fibrous amoeboid (activated) shapes of microglia were observed (Figs. 4–6). Administration of CP-101,606 after SE onset did not alter Iba1$^+$/ED1$^+$ double-labeling profile in comparison to SE + SAL group in all regions analyzed. However, animals from both SE + KET and SE + CI groups presented a reduction in the Iba1$^+$ cells in CA1 [$F(3,23) = 9.24$; $P = 0.0003$] and MePV [$F(3,22) = 22.51$; $P < 0.0001$], but not in DG [$F(3,23) = 0.96$; $P = 0.43$] (Fig. 7a–c). In addition, both groups displayed a reduction in the number of ED1$^+$ cells in CA1 [$F(3,23) = 14.46$; $P < 0.0001$] and MePV [$F(3,22) = 14.70$; $P < 0.0001$] (Fig. 7d and f). Significant reduction of activated microglia was also observed in these regions when the percentage of ED1$^+$ cell in relation to the total number of Iba1$^+$ cells was analyzed [$F(3,23) = 15.70$; $P < 0.0001$ for CA1; $F(3,22) = 7.08$; $P < 0.0017$ for MePV] (Fig. 7g and i). One-way ANOVA also revealed a significant difference between groups in the total number of ED1$^+$ cells in DG [$F(3,23) = 3.37$; $P = 0.0359$]. Nevertheless, Holm-Sidak's post hoc test for multiple comparisons was not able to identify differences between groups ($P = 0.0611$ for SE + SAL *vs.* SE + KET; $P = 0.1417$ for SE + SAL *vs.* SE + CI; $P = 0.9477$ for SE + SAL *vs.* SE + CP), just pointing a trend of SE + KET group for reducing ED1$^+$ cells in comparison to SE + SAL group. This suggested reduction of microglial activation in DG was strengthened by the reduction observed in the percentage of ED1$^+$ cells in relation to the total number of Iba1$^+$ cells [$F(3,23) = 4.67$; $P = 0.0109$] (Fig. 7h). Even though microglial morphology was not evaluated (quantified) it is clear that ramified cells

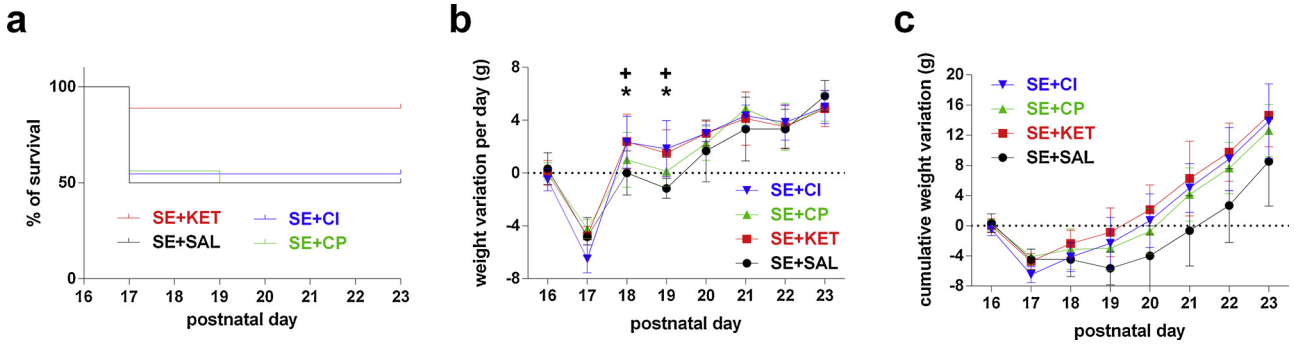

Fig. 2. Blockage of GluN2B-containing NMDAR effects on time-course mortality and weight recovery after SE induction at PND16. (a) Data of mortality are expressed as the total N for each group (SE + SAL $N = 12$; SE + KET $N = 9$; SE + CP $N = 16$; SE + CI $N = 11$) and were analyzed by Mantel–Cox test. (b) Body weight variation per day was calculated as PNDn-(PNDn-1); *e.g.* PND17-(PND16). Values near from 0 (dotted line) indicates that animals did not gain weight in that day; negative values indicates that animals lose weight in that day; positive values indicates that animals gain weight in that day. (c) Cumulative body weight variation was calculated as PNDn-PND15. Values were normalized by the body weight each animal had in PND15 (dotted line). * indicates $P < 0.05$ when SE + KET group was compared with SE + SAL group. + indicates $P < 0.05$ when SE + CI group was compared with SE + SAL group. Data of body weight variation per day were analyzed by two-way ANOVA with repeated measures followed by Holm-Sidak's multiple comparisons post hoc test.

were the majority shape of microglial cells found in SE + KET and SE + CI groups (Figs. 4–6), which supports the hypothesis that NMDAR-antagonism reduces microglial activation induced by SE.

4. Discussion

The results presented herein showed that GluN2B-containing NMDAR are involved in neuronal loss and microglial recruitment and activation caused by early-life SE. As we predicted, SE-induced neurodegeneration and microglial recruitment and activation were substantially reduced (fully avoided in most cases) after blocking GluN2B-containing NMDAR with CI-1041. However, our hypothesis that excessive activation of extrasynaptic NMDAR is the mechanism responsible for SE-induced neurodegeneration was not confirmed since

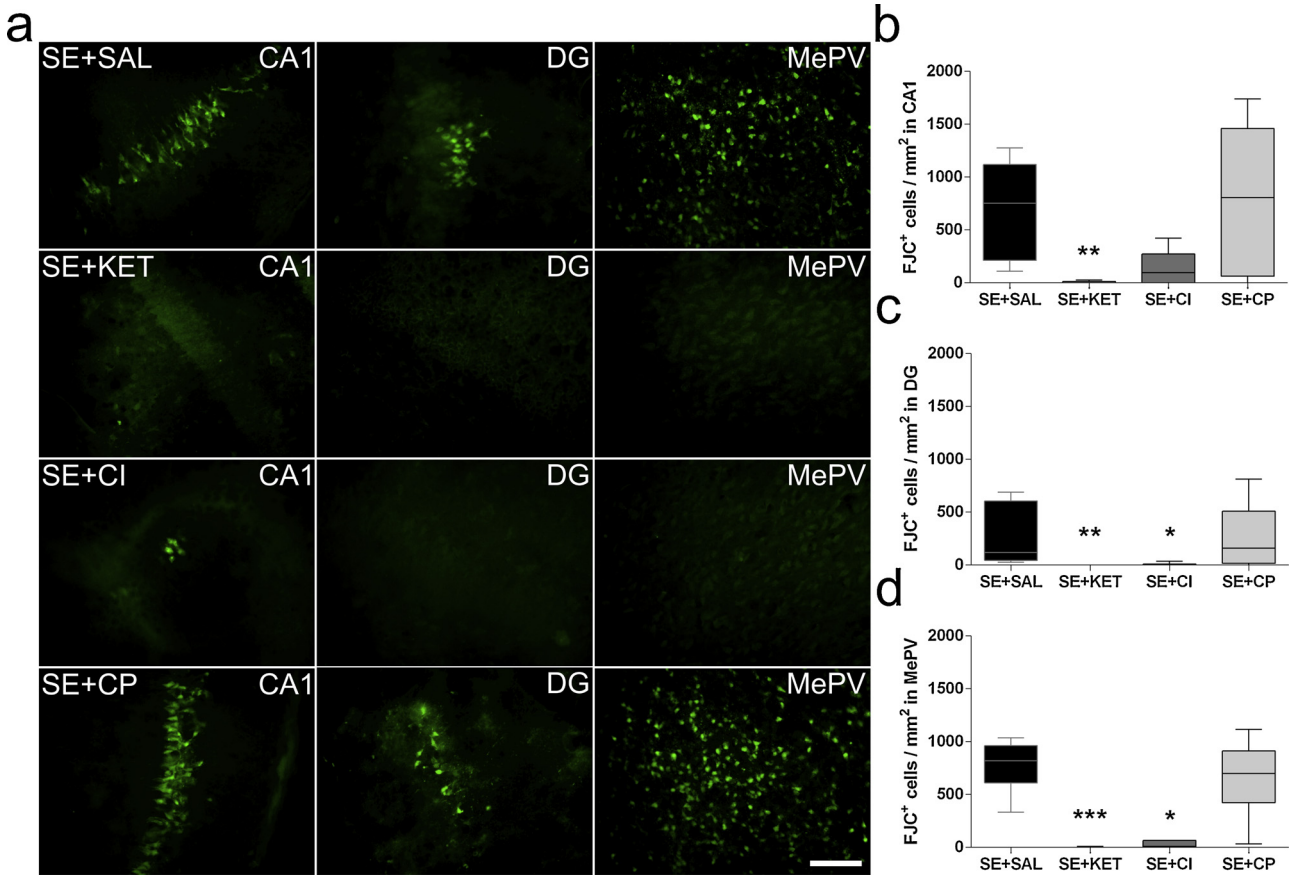

Fig. 3. Blockage of GluN2B-containing NMDAR with CI-1041 prevents SE-induced neurodegeneration. (a) Representative images from FJC labeling performed seven days after SE onset. SE induced a massive neurodegeneration in several brain regions, including CA1 hippocampal subfield (left), DG hippocampal subfield (middle) and medial amygdaloid nucleus (MePV; right). Scale bar = 100 µm. (b–d) In the graphs are depicted the quantification of FJC^+ neurons in (b) CA1 and (c) DG hippocampal subfields, and (d) amygdala (medial amygdaloid nucleus - MePV), seven days after SE onset. Data were analyzed by Kruskal-Wallis test followed by Dunn's multiple comparisons post hoc test. * indicates $P < 0.05$ when compared with SE + SAL group. ** indicates $P < 0.01$ when compared with SE + SAL group. *** indicates $P < 0.001$ when compared with SE + SAL group.

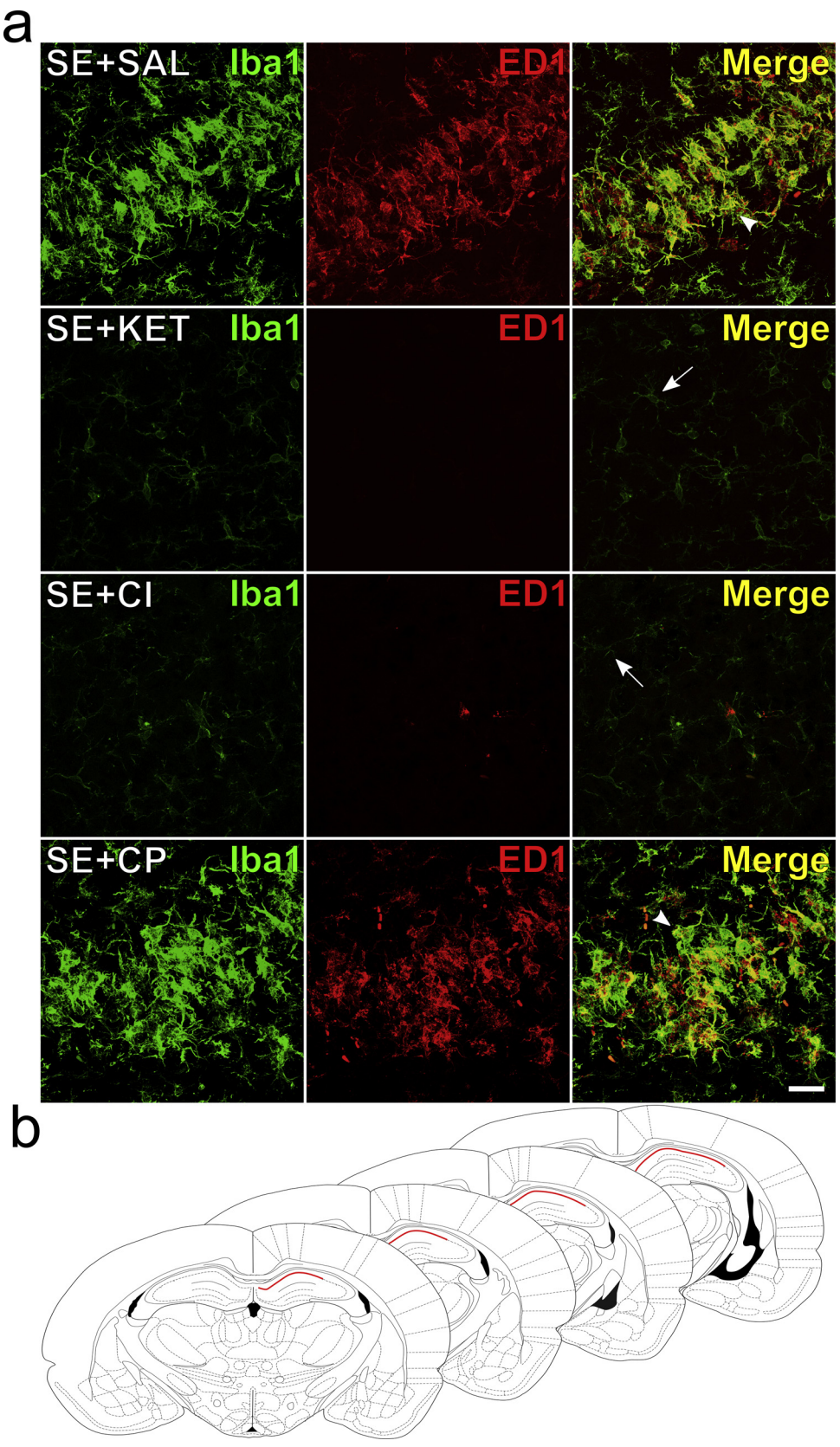

Fig. 4. Microglial recruitment and activation in the CA1 hippocampal subfield seven days after SE onset. (a) SE induced a massive microglial recruitment (Iba1$^+$ cells; green) and activation (ED1$^+$ cells; red) in the CA1 hippocampal subfield. Coronal sections show a markedly decreased number of Iba1$^+$ and ED1$^+$ double-labeled cells from SE + KET and SE + CI, but not from SE + CP, treated animals when compared with SE + SAL group. A higher incidence of yellowish-green cells indicates Iba1/ED1 co-localization. Ramified (resting - arrows) and fibrous amoeboid (activated – arrow heads) shapes of microglia were observed. Scale bar = 25 µm. (b) Representative coronal sections of the regions analyzed (from Bregma -3.14 mm to -3.80 mm). CA1 hippocampal subfield is highlighted in red. Modified of Paxinos and Watson (1998). (For interpretation of the references to colour in this figure legend, the reader is referred to the web version of this article.)

selective blockade of NMDAR composed by GluN1/GluN2B diheteromers, with CP-101,606 (Chazot et al., 2002; Hansen et al., 2014), did not prevent neuronal loss. Our results also suggest a decoupling of brain damage and epileptic activity since we showed that stopping SE is not required to prevent neurodegeneration and microglial recruitment and activation. In the following sections, we provide experimental evidence supporting our findings and propose putative mechanisms involved in NMDAR-mediated glutamatergic excitotoxicity.

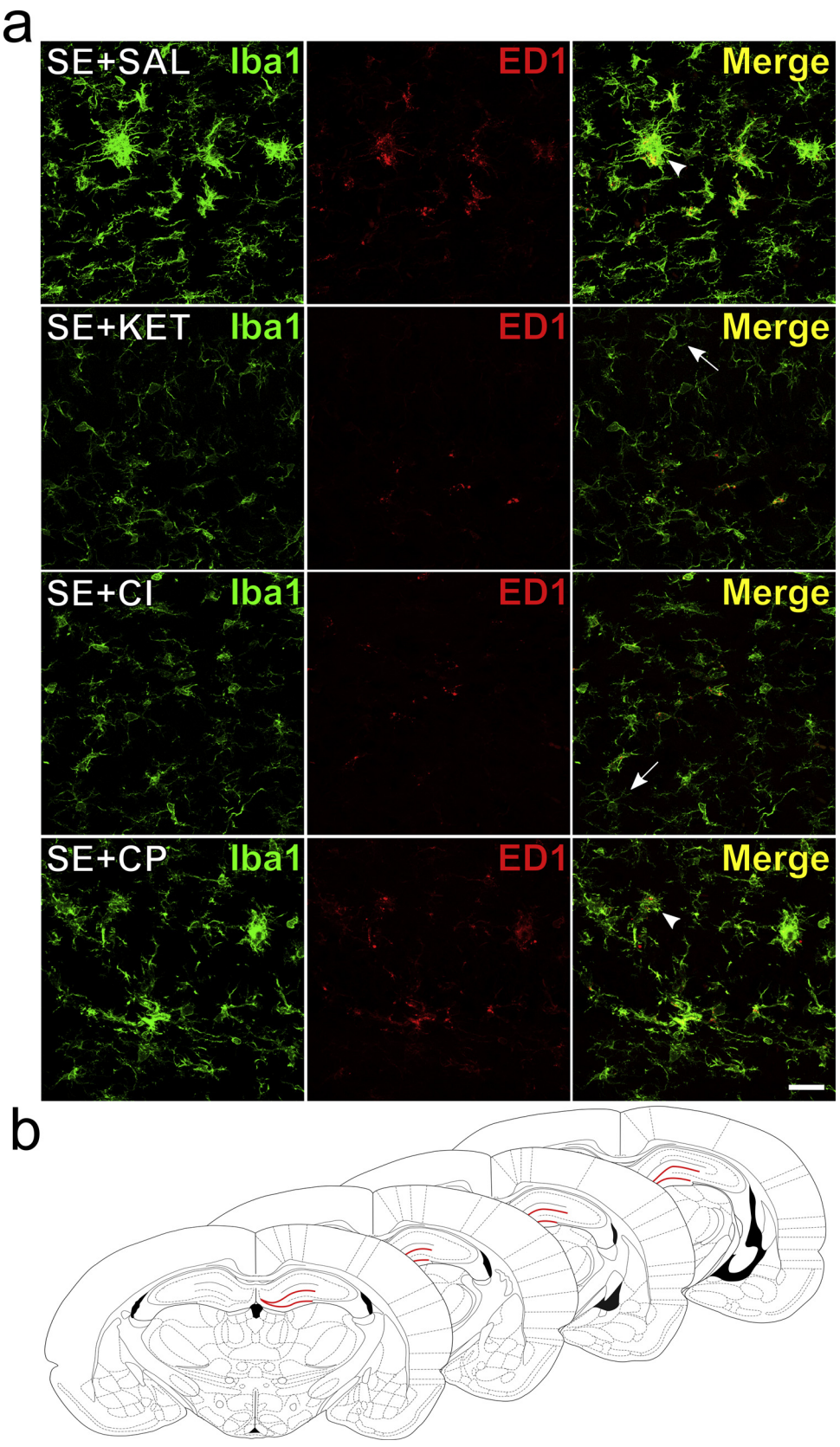

Fig. 5. Microglial recruitment and activation in the DG hippocampal subfield seven days after SE onset. (a) SE induced a massive microglial recruitment (Iba1$^+$ cells; green) and activation (ED1$^+$ cells; red) in the DG hippocampal subfield. Coronal sections show a markedly difference in shape of Iba1$^+$ and ED1$^+$ double-labeled cells from SE + KET and SE + CI, but not from SE + CP, treated animals when compared with SE + SAL group. A higher incidence of yellowish-green cells indicates Iba1/ED1 co-localization. Ramified (resting - arrows) and fibrous amoeboid (activated – arrow heads) shapes of microglia were observed. Scale bar = 25 µm. (b) Representative coronal sections of the regions analyzed (from Bregma -3.14 mm to -3.80 mm). DG hippocampal subfield is highlighted in red. Modified of Paxinos and Watson (1998). (For interpretation of the references to colour in this figure legend, the reader is referred to the web version of this article.)

4.1. Blockade of GluN2B-containing NMDAR with CP-101,606 or CI-1041 failed to stop LiCl-pilocarpine-induced SE

It is well-known that typical NMDAR antagonists exhibit potent anticonvulsant activity (Mikolasova et al., 1994; Velisek et al., 1989; Veliskova et al., 1990). Recent evidence points to the involvement of GluN2B subunit in maintenance of seizures since blockade of GluN2B-containing NMDAR can suppress epileptic activity (Brackett et al., 2000; Mares and Mikulecka, 2009; Szczurowska and Mares, 2015; Wang and Bausch, 2004). However, in our study, blockade of GluN2B-

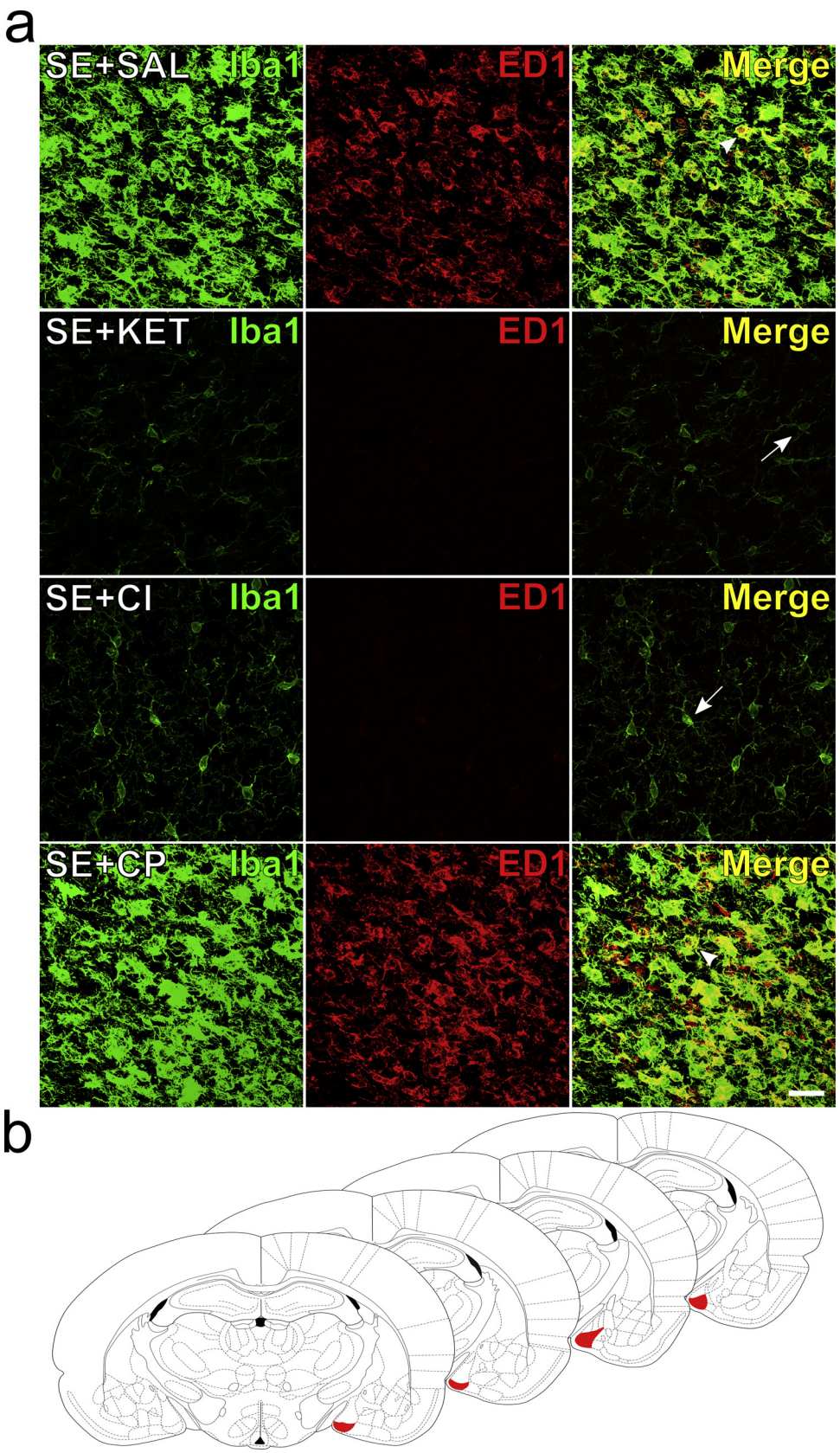

Fig. 6. Microglial recruitment and activation in amygdala seven days after SE onset. (a) SE induced a massive microglial recruitment ($Iba1^+$ cells; green) and activation ($ED1^+$ cells; red) in the medial amygdaloid nucleus (MePV). Coronal sections show a markedly decreased number of $Iba1^+$ and $ED1^+$ double-labeled cells from SE + KET and SE + CI, but not from SE + CP, treated animals when compared with SE + SAL group. A higher incidence of yellowish-green cells indicates Iba1/ED1 co-localization. Ramified (resting - arrows) and fibrous amoeboid (activated – arrow heads) shapes of microglia were observed. Scale bar = 25 µm. (b) Representative coronal sections of the regions analyzed (from Bregma -2.56 mm to -3.30 mm). MePV is highlighted in red. Modified of Paxinos and Watson (1998). (For interpretation of the references to colour in this figure legend, the reader is referred to the web version of this article.)

containing NMDAR with CP-101,606 or CI-1041 did not stop SE-induced seizures. This was a surprising result since others previously reported anticonvulsant activity of these antagonists in higher, similar or even lower dosage than the used here (Barton and White, 2004; Brackett et al., 2000; Naspolini et al., 2012; Vartanian et al., 2000). One can argue that GluN2B-containing NMDAR antagonism present different anticonvulsant actions in adult and developmental brain. Nevertheless, anticonvulsant effect of GluN2B-containing NMDAR

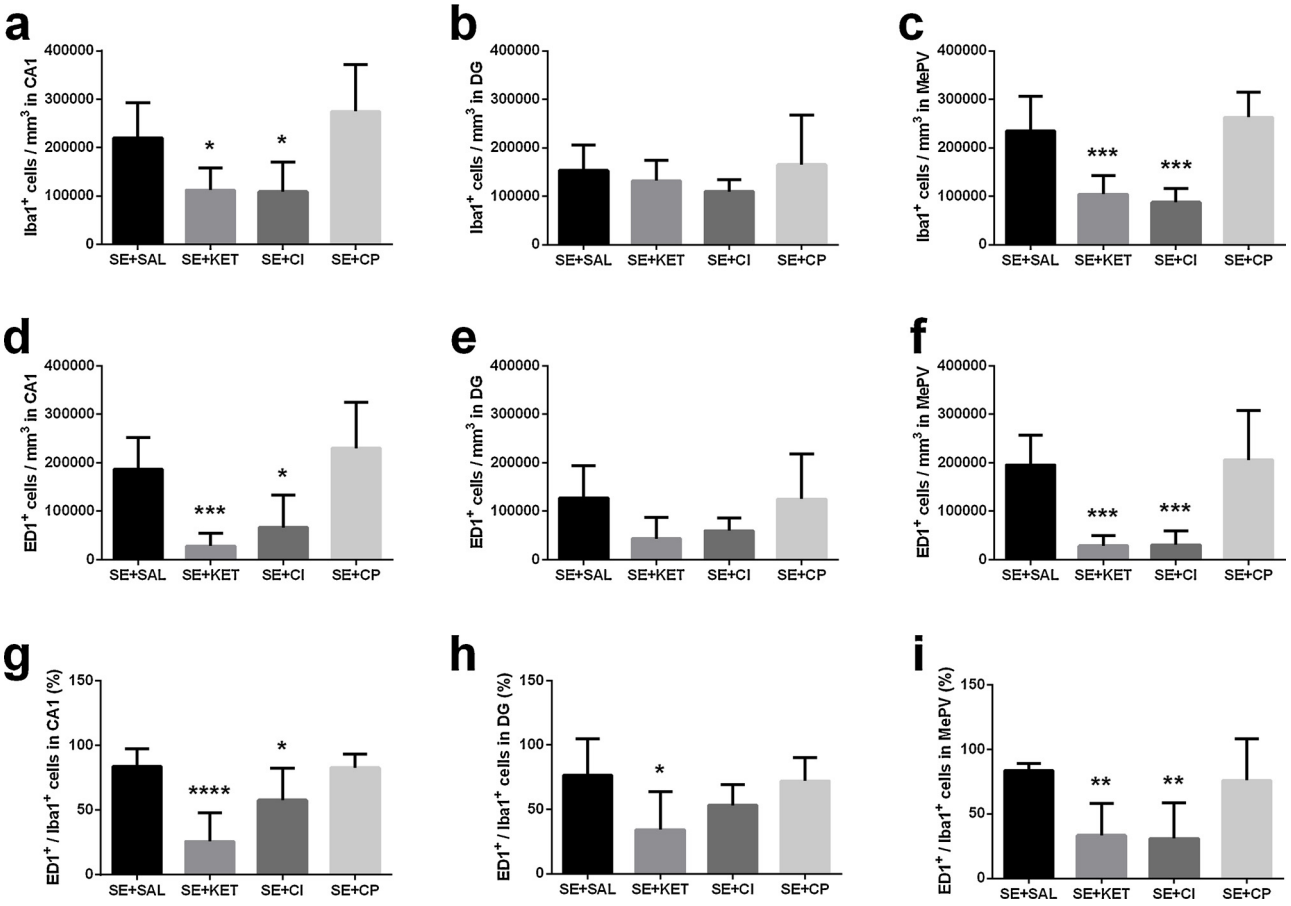

Fig. 7. Blockage of GluN2B-containing NMDAR with CI-1041 prevents SE-induced microglial recruitment and activation. (Top) Quantification of Iba1$^+$ in (a) CA1, (b) DG and (c) amygdala (medial amygdaloid nucleus - MePV) seven days after SE onset. (Middle) Quantification of ED1$^+$ cells in (d) CA1, (e) DG and (f) MePV seven days after SE onset. (Bottom) Ratio between ED1$^+$ cells and Iba1$^+$ cells (calculated as ED1$^+$ cells divided by Iba1$^+$ cells multiplied by 100) in (g) CA1, (h) DG and (i) MePV. Data were analyzed by One-Way ANOVA followed by Holm-Sidak's multiple comparisons post hoc test. * indicates $P < 0.05$ when compared with SE + SAL group. ** indicates $P < 0.01$ when compared with SE + SAL group. *** indicates $P < 0.001$ when compared with SE + SAL group. **** indicates $P < 0.0001$ when compared with SE + SAL group.

antagonists was already reported in both adult and immature rats (Mares and Mikulecka, 2009; Naspolini et al., 2012; Szczurowska and Mares, 2015). We believe that the most plausible explanation for these contrasting results is the different models used to induce seizures. Anticonvulsant effects of CI-1041 was observed in corneal-kindling seizures and sound-induced seizures but not in amygdala-kindled seizures (Barton and White, 2004; Vartanian et al., 2000), while protective effects of CP-101,606 was only reported in cocaine-induced seizures (Brackett et al., 2000) and pentylenetetrazol-induced seizures (Naspolini et al., 2012). Based on the above cited data, plus the inefficacy of both CP-101,606 and CI-1041 in stopping LiCl-pilocarpine-induced SE in our study, we believe that GluN2B-containing NMDAR antagonists are not yet ready to be used as anticonvulsant drugs.

4.2. Blockade of GluN2B-containing NMDAR with CI-1041 accelerates weight recovery after SE

In agreement with previous reports (de Oliveira et al., 2008; Loss et al., 2012), rats submitted to SE showed a significant weight loss 24 h after SE onset. Animals treated with ketamine during SE displayed faster weight recovery, as seen in previous unpublished data from our group. Since the excessive activity of the nervous and muscular systems during SE can lead to depletion of energy reserves (Lothman, 1990; Michelson-Kerman et al., 2003), one can argue that acceleration of weight recovery on ketamine-treated animals is related to a reduced depletion in their energy reserves because motor activity (and probably epileptic activity) was terminated after ketamine injection. However, weight loss was similar between groups 24 h after SE onset (Fig. 2b). On the other hand, weight gain was accelerated on the following days for both SE + KET and SE + CI groups, suggesting that duration of postictal period was reduced by GluN2B-containing NMDAR antagonism during SE. Accordingly to previous reports, GluN2B-containing NMDAR antagonism provided a good recovery for individuals suffering brain injury, such as severe head trauma or seizures (Chazot, 2000; Mares and Mikulecka, 2009). Therefore, treatment with CI-1041 seems to be neuroprotective against SE even in a lack of anticonvulsant effect.

4.3. Blockade of GluN2B-containing NMDAR with CI-1041 prevents SE-induced brain damage

SE during brain development may cause acute brain damage (Holmes, 1997; van Esch et al., 1996) which is frequently associated to over-activation of NMDAR and subsequent glutamatergic excitotoxicity (Clifford et al., 1990; Fariello et al., 1989; Fujikawa, 1995; Sankar et al., 1998). In agreement with previous works (de Oliveira et al., 2008; Sankar et al., 1998), early-life SE induced an extensive neuronal death accompanied by pronounced microgliosis (indicated by the increased microglial recruitment and activation) in CA1 and DG subfields of hippocampus and also in MePV amygdaloid nucleus. SE-induced neurodegeneration was prevented by post-SE onset administration of ketamine (Loss et al., 2012), which was accompanied by prevention of microglial recruitment and activation in all regions analyzed.

Evidence points to a hypothesis that neuronal death pathways are related to Ca^{2+} influx trough extrasynaptic NMDAR (Hardingham and Bading, 2010; Hardingham et al., 2002), which are mostly GluN1/GluN2B diheteromers. However, in our study, post-SE onset administration of CP-101,606, a NMDAR antagonist with great selectivity for GluN1/GluN2B diheteromers (Chazot et al., 2002; Hansen et al., 2014), was not effective in prevent both neurodegeneration and microglial recruitment and activation induced by SE. On the other hand, post-SE onset treatment with GluN2B-containing NMDAR antagonist, CI-1041, reduced neurodegeneration and microglial recruitment and activation similarly to post-SE onset treatment with ketamine. Our results indicate differences in the pharmacological properties and/or mechanism of action between the two NMDAR antagonists CP-101,606 and CI-1041. In fact, evidence for two classes of selective GluN2B-containing NMDAR antagonists was already proposed by Chazot et al. (2002), which demonstrated that CP-101,606 binding is affected significantly by the presence of another GluN2 subunit type within the receptor complex, while a second class of selective GluN2B-containing NMDAR antagonists, exemplified by Ro-25,6981 in the above cited study, binds to NMDAR with high affinity irrespective whether another GluN2 subunit type is present. Despite the considerable resources used in the characterization of GluN2B-containing NMDAR antagonist CI-1041 (Coughenour et al., 2000; Kovacs et al., 2004; Nagy et al., 2004; Whittemore et al., 2000), there is a problematic lack of information regarding its activity at NMDAR composed by GluN1/GluN2A/GluN2B triheteromers (or other possible types of NMDAR triheteromeric containing the GluN2B subunit). Our results highly suggest that CI-1041 is more likely to Ro-25,6981's class of GluN2B-containing NMDAR antagonists, and that its neuroprotective effects could be related not only to the receptor subtype that is blocked (NMDAR composed by GluN1/GluN2A/GluN2B triheteromers, for instance) but also to the increased percentage of the full NMDAR population that is blockade (*i.e.*, blocking more NMDAR is likely to be more neuroprotective). Thus, neuroprotective effects of CI-1041 plus the inefficacy of CP-101,606 in preventing SE-induced brain damage indicates that over-activation of NMDAR composed by GluN1/GluN2B diheteromers is not the main mechanism involved in NMDAR-mediated neurodegeneration and neuroinflammation induced by SE.

Regarding the relationship between SE, excitotoxicity and neuroinflammation, two hypotheses come to light to explain our results: (i) SE-induced microgliosis is occurring in response to neuronal death and not due to epileptic activity or neuronal hyperexcitability *per se*; or (ii) absence of microgliosis in animals treated with CI-1041 after SE onset could be related to direct inhibition of microglial NMDAR. Whether the first hypothesis is true, post-SE onset administration of CI-1041 was effective in avoid neurodegeneration, which prevented subsequently microglial activation. Importantly, this neuroprotection was observed even in a lack of anticonvulsive effect of CI-1041. These hypothesis are in accordance with the argument that microgliosis seen after SE may be linked to the need for clearing the apoptotic cells (Schartz et al., 2016; Wyatt-Johnson et al., 2017), which are absent after post-SE onset CI-1041 administration. In favor of the second hypothesis, one can argue that direct activation of microglial NMDAR can also triggers glutamatergic excitotoxicity inducing an inflammation/neurodegeneration vicious cycle (Kaindl et al., 2012), and that this phenomenon was prevented through direct inhibition of microglial NMDAR by CI-1041. To elucidate if after SE, microgliosis is provoking neurodegeneration or vice versa further investigation is needed.

4.4. SE-induced neurodegeneration through synaptic and extrasynaptic NMDAR co-activation hypothesis

The current most accepted theory of NMDAR-mediated neurodegeneration postulates that over-activation of extrasynaptic NMDAR counteracts synaptic NMDAR and triggers cell death (Hardingham and Bading, 2010; Hardingham et al., 2002). However, an important methodological issue limits the full acceptance of this theory. Most studies proposing neuronal death mediated by extrasynaptic NMDAR activation have suggested this mechanism after using bath application of NMDA (or glutamate), which is known to activate both synaptic and extrasynaptic NMDAR (Hardingham et al., 2002; Zhou et al., 2013). In contrast to the current prevailing theory, a glutamatergic excitotoxicity through synaptic and extrasynaptic NMDAR co-activation hypothesis has been proposed (Chen et al., 2014; Zhou et al., 2013). Zhou et al. (2013) extensively demonstrated that NMDAR activation trough synaptic- or extrasynaptic stimulation alone did not lead neurons to death. On the other hand, neuronal death was observed when both synaptic and extrasynaptic NMDAR were simultaneously activated (Chen et al., 2014; Zhou et al., 2013). Also, they observed that transient co-activation of synaptic- and extrasynaptic-NMDAR did not cause cell death, suggesting that magnitude of co-activation of these receptors determines the degree of cell death. Our results are in accordance with the NMDAR co-activation hypothesis since blocking only the sub-population of NMDAR composed by GluN1/GluN2B diheteromers did not prevent neuronal death. Instead, blocking the full GluN2B-containing NMDAR population (including GluN1/GluN2B diheteromers), with CI-1041, prevented neurodegeneration and subsequent microglial recruitment and activation. Together our results suggest that synaptic and extrasynaptic (non-GluN1/GluN2B diheteromers) GluN2B-containing NMDAR activation are required to trigger SE-induced neurodegeneration. Evidences that activation of synaptic NMDAR takes part in neuronal death under pathological conditions give further support to this hypothesis (Papouin et al., 2012; Sattler et al., 2000; Wroge et al., 2012).

4.5. Methodological issues and study limitations

Although our data are robust and allow us to conclude that blockade of GluN2B-containing NMDAR reduces short-term brain damage induced by early-life SE, there are some methodological issues that deserves to be discussed. In our study, both sexes were used and data were analyzed without distinction between male and female individuals. One can argue that sexual dimorphism in NMDAR-mediated responses could be affecting the data. However, most sex differences in NMDAR expression and composition are observed in adults or at very early stages of brain development (first postnatal week). The evidence points to absence of sexual dimorphism in NMDAR expression and composition in PND16 (the period we subject the animals to SE) or even around this stage of brain development (second and third postnatal weeks) (Damborsky and Winzer-Serhan, 2012; Tavassoli et al., 2013). Moreover, sexual dimorphism in mortality rate was not observed ($P = 0.77$; data not shown), and a similar proportion of males and females (about 50%) was maintained in each experimental group to minimize a putative influence of sex on our findings.

Another methodological issue that deserves attention is the criteria we used for stereological analysis in hippocampus. One can argue that by purposely selecting the most damage region for analysis, data could be biased away from the null. In fact, due to the anisotropic nature of the distributions of neurodegeneration and microgliosis in CA1 and DG, both strategies of randomly assign a portion of the region, or purposely selecting a region for analysis would lead to a miss estimation of the damage. Once our aim was to investigate whether blockade of GluN2B-containing NMDAR would prevent brain damaged induced by early-life SE, we choose to minimize the chance of mistakenly interpreting that tested compounds were neuroprotective when they were not, therefore increasing the chance of mistakenly inferring that the tested compounds did not present neuroprotective effects when they actually did. Importantly, even by purposely selecting the most damaged regions (which could lead to an overestimation of cell densities in SE + KET and SE + CI groups), neurodegeneration and microgliosis were evidently reduced in these groups.

5. Conclusion

In summary, we showed in the present study that GluN2B-containing NMDAR antagonism by CP-101,606 and CI-1041 was not able to stop seizures neither to reduce weight loss nor mortality after LiCl-pilocarpine-induced SE. However, blockade of GluN2B-containing NMDAR accelerated weight recovery and prevented neuronal death and neuroinflammation in the immature brain. Moreover, by putatively using two classes of selective GluN2B-containing NMDAR antagonists our results suggest that NMDAR composed by GluN1/GluN2B diheteromers are not the major sub-population involved in NMDAR-mediated neurodegeneration and neuroinflammation induced by SE. Instead, the NMDAR sub-population composed by GluN1/GluN2A/GluN2B triheteromers probably plays a key role in these processes. Nevertheless, further investigation will be required to fully understand the cellular and neurochemical mechanisms involved in SE-induced neurodegeneration and neuroinflammation.

Funding sources

This work was supported by the Brazilian funding agencies, Conselho Nacional de Desenvolvimento Científico e Tecnológico (CNPq) [Edital Doenças Neurodegenerativas/Processo No. 467676/2014-3]; Fundação de Amparo à Pesquisa do Estado do Rio Grande do Sul - FAPERGS/PRONEX [16/2551-0000499-4]; Coordenação de Aperfeiçoamento de Pessoal de Nível Superior (CAPES); and UFRGS/Propesq.

Conflict of interest

The authors declare that Pfizer Inc. (USA) has donated CP-101,606 and CI-1041 drugs used in this work. We further affirm that none of the authors have any association with Pfizer Inc. or any other institution that may characterize a conflict of interest and affect the results or conclusions presented in this study.

Transparency document

The Transparency document associated with this article can be found in the online version.

Acknowledgements

This work was supported by the Brazilian funding agencies, CNPq [Edital Doenças Neurodegenerativas/Processo No. 467676/2014-3], FAPERGS/PRONEX [16/2551-0000499-4], CAPES and UFRGS/Propesq. The authors are grateful to Pfizer Inc. (USA) for kindly donation of CP-101,606 and CI-1041 drugs. We are also grateful to Camila Dias for providing language assistance.

References

Barton, M.E., White, H.S., 2004. The effect of CGX-1007 and CI-1041, novel NMDA receptor antagonists, on kindling acquisition and expression. Epilepsy Res. 59 (1), 1–12. https://doi.org/10.1016/j.eplepsyres.2003.12.010. S092012110400049X [pii].

Bertoglio, D., Amhaoul, H., Van Eetveldt, A., Houbrechts, R., Van De Vijver, S., Ali, I., Dedeurwaerdere, S., 2017. Kainic acid-induced post-status epilepticus models of temporal lobe epilepsy with diverging seizure phenotype and neuropathology. Front. Neurol. 8, 588. https://doi.org/10.3389/fneur.2017.00588.

Brackett, R.L., Pouw, B., Blyden, J.F., Nour, M., Matsumoto, R.R., 2000. Prevention of cocaine-induced convulsions and lethality in mice: effectiveness of targeting different sites on the NMDA receptor complex. Neuropharmacology 39 (3), 407–418.

Chazot, P.L., 2000. CP-101606 pfizer inc. Curr. Opin. Investig. Drugs 1 (3), 370–374.

Chazot, P.L., Lawrence, S., Thompson, C.L., 2002. Studies on the subtype selectivity of CP-101,606: evidence for two classes of NR2B-selective NMDA receptor antagonists. Neuropharmacology 42 (3), 319–324.

Chen, L.R., Wesley, J.A., Bhattachar, S., Ruiz, B., Bahash, K., Babu, S.R., 2003. Dissolution behavior of a poorly water soluble compound in the presence of Tween 80. Pharm. Res. 20 (5), 797–801.

Chen, Z., Zhou, Q., Zhang, M., Wang, H., Yun, W., Zhou, X., 2014. Co-activation of synaptic and extrasynaptic NMDA receptors by neuronal insults determines cell death in acute brain slice. Neurochem. Int. 78, 28–3410.

Choi, J., Koh, S., 2008. Role of brain inflammation in epileptogenesis. Yonsei Med. J. 49 (1), 1–1810.

Clifford, D.B., Olney, J.W., Benz, A.M., Fuller, T.A., Zorumski, C.F., 1990. Ketamine, phencyclidine, and MK-801 protect against kainic acid-induced seizure-related brain damage. Epilepsia 31 (4), 382–390.

Costa-Ferro, Z.S., Vitola, A.S., Pedroso, M.F., Cunha, F.B., Xavier, L.L., Machado, D.C., Soares, M.B., Ribeiro-dos-Santos, R., DaCosta, J.C., 2010. Prevention of seizures and reorganization of hippocampal functions by transplantation of bone marrow cells in the acute phase of experimental epilepsy. Seizure 19 (2), 84–92. https://doi.org/10.1016/j.seizure.2009.12.003. S1059-1311(09)00246-5 [pii].

Coughenour, L.L., Barr, B., Espitia, S., Pugsley, T.A., Whetzel, S.Z., Dooley, D., Mieske, C., Ilyin, V., Rock, D.M., Stoehr, S., Boxer, P.A., 2000. Neurochemical Pharmacology of CI-1041 (PD196860): a Novel Subtype Selective NMDA Antagonist. Program No. 527.4. Neuroscience Meeting Planner. Society for Neuroscience, New Orleans, LA 2000, Online. Abstr.

Dall'Oglio, A., Xavier, L.L., Hilbig, A., Ferme, D., Moreira, J.E., Achaval, M., Rasia-Filho, A.A., 2013. Cellular components of the human medial amygdaloid nucleus. J. Comp. Neurol. 521 (3), 589–611. https://doi.org/10.1002/cne.23192.

Damborsky, J.C., Winzer-Serhan, U.H., 2012. Effects of sex and chronic neonatal nicotine treatment on Na(2)(+)/K(+)/Cl(-) co-transporter 1, K(+)/Cl(-) co-transporter 2, brain-derived neurotrophic factor, NMDA receptor subunit 2A and NMDA receptor subunit 2B mRNA expression in the postnatal rat hippocampus. Neuroscience 225, 105–117. https://doi.org/10.1016/j.neuroscience.2012.09.002. S0306-4522(12)00904-9 [pii].

de Oliveira, D.L., Fischer, A., Jorge, R.S., da Silva, M.C., Leite, M., Goncalves, C.A., Quillfeldt, J.A., Souza, D.O., e Souza, T.M., Wofchuk, S., 2008. Effects of early-life LiCl-pilocarpine-induced status epilepticus on memory and anxiety in adult rats are associated with mossy fiber sprouting and elevated CSF S100B protein. Epilepsia 49 (5), 842–852. https://doi.org/10.1111/j.1528-1167.2007.01484.x. EPI1484 [pii].

de Senna, P.N., Bagatini, P.B., Galland, F., Bobermin, L., do Nascimento, P.S., Nardin, P., Tramontina, A.C., Goncalves, C.A., Achaval, M., Xavier, L.L., 2017. Physical exercise reverses spatial memory deficit and induces hippocampal astrocyte plasticity in diabetic rats. Brain Res. 1655, 242–251 S0006-8993(16)30728-4 [pii].

Di Maio, R., Mastroberardino, P.G., Hu, X., Montero, L., Greenamyre, J.T., 2011. Pilocapine alters NMDA receptor expression and function in hippocampal neurons: NADPH oxidase and ERK1/2 mechanisms. Neurobiol. Dis. 42 (3), 482–495. https://doi.org/10.1016/j.nbd.2011.02.012. S0969-9961(11)00066-0 [pii].

Ekdahl, C.T., Claasen, J.H., Bonde, S., Kokaia, Z., Lindvall, O., 2003. Inflammation is detrimental for neurogenesis in adult brain. Proc. Natl. Acad. Sci. U. S. A. 100 (23), 13632–13637. https://doi.org/10.1073/pnas.2234031100.

Fariello, R.G., Golden, G.T., Smith, G.G., Reyes, P.F., 1989. Potentiation of kainic acid epileptogenicity and sparing from neuronal damage by an NMDA receptor antagonist. Epilepsy Res. 3 (3), 206–213.

Fujikawa, D.G., 1995. Neuroprotective effect of ketamine administered after status epilepticus onset. Epilepsia 36 (2), 186–195.

Gladding, C.M., Raymond, L.A., 2011. Mechanisms underlying NMDA receptor synaptic/extrasynaptic distribution and function. Mol. Cell. Neurosci. 48 (4), 308–320. https://doi.org/10.1016/j.mcn.2011.05.001. S1044-7431(11)00107-2 [pii].

Gross-Tsur, V., Shinnar, S., 1993. Convulsive status epilepticus in children. Epilepsia 34 (Suppl. 1), S12–20.

Hansen, K.B., Ogden, K.K., Yuan, H., Traynelis, S.F., 2014. Distinct functional and pharmacological properties of Triheteromeric GluN1/GluN2A/GluN2B NMDA receptors. Neuron 81 (5), 1084–1096. https://doi.org/10.1016/j.neuron.2014.01.035. S0896-6273(14)00066-X [pii].

Hardingham, G.E., Bading, H., 2010. Synaptic versus extrasynaptic NMDA receptor signalling: implications for neurodegenerative disorders. Nat. Rev. Neurosci. 11 (10), 682–696. https://doi.org/10.1038/nrn2911. nrn2911 [pii].

Hardingham, G.E., Fukunaga, Y., Bading, H., 2002. Extrasynaptic NMDARs oppose synaptic NMDARs by triggering CREB shut-off and cell death pathways. Nat. Neurosci. 5 (5), 405–414. https://doi.org/10.1038/nn835. nn835 [pii].

Holmes, G.L., 1997. Epilepsy in the developing brain: lessons from the laboratory and clinic. Epilepsia 38 (1), 12–30.

Holmes, G.L., 2004. Effects of early seizures on later behavior and epileptogenicity. Ment. Retard. Dev. Disabil. Res. Rev. 10 (2), 101–105. https://doi.org/10.1002/mrdd.20019.

Holopainen, I.E., 2008. Seizures in the developing brain: cellular and molecular mechanisms of neuronal damage, neurogenesis and cellular reorganization. Neurochem. Int. 52 (6), 935–947 S0197-0186(07)00308-7 [pii].

Jakubs, K., Nanobashvili, A., Bonde, S., Ekdahl, C.T., Kokaia, Z., Kokaia, M., Lindvall, O., 2006. Environment matters: synaptic properties of neurons born in the epileptic adult brain develop to reduce excitability. Neuron 52 (6), 1047–1059 S0896-6273(06)00870-1 [pii].

Kaindl, A.M., Degos, V., Peineau, S., Gouadon, E., Chhor, V., Loron, G., Le Charpentier, T., Josserand, J., Ali, C., Vivien, D., Collingridge, G.L., Lombet, A., Issa, L., Rene, F., Loeffler, J.P., Kavelaars, A., Verney, C., Mantz, J., Gressens, P., 2012. Activation of microglial N-methyl-D-aspartate receptors triggers inflammation and neuronal cell death in the developing and mature brain. Ann. Neurol. 72 (4), 536–549. https://doi.org/10.1002/ana.23626.

Kovacs, G., Kocsis, P., Tarnawa, I., Horvath, C., Szombathelyi, Z., Farkas, S., 2004. NR2B containing NMDA receptor dependent windup of single spinal neurons. Neuropharmacology 46 (1), 23–30 S0028390803003393 [pii].

Kubova, H., Mares, P., Suchomelova, L., Brozek, G., Druga, R., Pitkanen, A., 2004. Status epilepticus in immature rats leads to behavioural and cognitive impairment and

epileptogenesis. Eur. J. Neurosci. 19 (12), 3255–3265. https://doi.org/10.1111/j.0953-816X.2004.03410.x. EJN3410 [pii].

Liu, H.J., Lai, X., Xu, Y., Miao, J.K., Li, C., Liu, J.Y., Hua, Y.Y., Ma, Q., Chen, Q., 2017. alpha-Asarone attenuates cognitive deficit in a pilocarpine-induced status epilepticus rat model via a decrease in the nuclear factor-kappaB activation and reduction in microglia neuroinflammation. Front. Neurol. 8, 661. https://doi.org/10.3389/fneur.2017.00661.

Loss, C.M., Cordova, S.D., de Oliveira, D.L., 2012. Ketamine reduces neuronal degeneration and anxiety levels when administered during early life-induced status epilepticus in rats. Brain Res. 1474, 110–117. https://doi.org/10.1016/j.brainres.2012.07.046. S0006-8993(12)01235-8 [pii].

Lothman, E., 1990. The biochemical basis and pathophysiology of status epilepticus. Neurology 40 (5 Suppl 2), 13–23.

Mares, P., Mikulecka, A., 2009. Different effects of two N-methyl-D-aspartate receptor antagonists on seizures, spontaneous behavior, and motor performance in immature rats. Epilepsy Behav. 14 (1), 32–39 S1525-5050(08)00259-X [pii].

Mestriner, R.G., Saur, L., Bagatini, P.B., Baptista, P.P., Vaz, S.P., Ferreira, K., Machado, S.A., Xavier, L.L., Netto, C.A., 2015. Astrocyte morphology after ischemic and hemorrhagic experimental stroke has no influence on the different recovery patterns. Behav. Brain Res. 278, 257–261. https://doi.org/10.1016/j.bbr.2014.10.005. S0166-4328(14)00653-6 [pii].

Michelson-Kerman, M., Watemberg, N., Nissenkorn, A., Gilad, E., Sadeh, M., Lerman-Sagie, T., 2003. Muscle glycogen depletion and increased oxidative phosphorylation following status epilepticus. J. Child Neurol. 18 (12), 876–878.

Mikolasova, R., Velisek, L., Vorlicek, J., Mares, P., 1994. Developmental changes of ketamine action against epileptic afterdischarges induced by hippocampal stimulation in rats. Brain Res. Dev. Brain Res. 81 (1), 105–112.

Mishra, V., Shuai, B., Kodali, M., Shetty, G.A., Hattiangady, B., Rao, X., Shetty, A.K., 2015. Resveratrol treatment after status epilepticus restrains neurodegeneration and abnormal neurogenesis with suppression of oxidative stress and inflammation. Sci. Rep. 5, 17807. https://doi.org/10.1038/srep17807. srep17807 [pii].

Nagy, J., Horvath, C., Farkas, S., Kolok, S., Szombathelyi, Z., 2004. NR2B subunit selective NMDA antagonists inhibit neurotoxic effect of alcohol-withdrawal in primary cultures of rat cortical neurones. Neurochem. Int. 44 (1), 17–23 S0197018603001001 [pii].

Naspolini, A.P., Cocco, A.R., Villa Martignoni, F., Oliveira, M.S., Furian, A.F., Rambo, L.M., Rubin, M.A., Barron, S., Mello, C.F., 2012. Traxoprodil decreases pentylenetetrazol-induced seizures. Epilepsy Res. 100 (1-2), 12–19. https://doi.org/10.1016/j.eplepsyres.2012.01.002. S0920-1211(12)00003-4 [pii].

Olney, J.W., 2003. Excitotoxicity, apoptosis and neuropsychiatric disorders. Curr. Opin. Pharmacol. 3 (1), 101–109 S1471489202000024 [pii].

Ouattara, B., Belkhir, S., Morissette, M., Dridi, M., Samadi, P., Gregoire, L., Meltzer, L.T., Di Paolo, T., 2009. Implication of NMDA receptors in the antidyskinetic activity of cabergoline, CI-1041, and Ro 61-8048 in MPTP monkeys with levodopa-induced dyskinesias. J. Mol. Neurosci. 38 (2), 128–142. https://doi.org/10.1007/s12031-008-9137-8.

Papouin, T., Ladepeche, L., Ruel, J., Sacchi, S., Labasque, M., Hanini, M., Groc, L., Pollegioni, L., Mothet, J.P., Oliet, S.H., 2012. Synaptic and extrasynaptic NMDA receptors are gated by different endogenous coagonists. Cell 150 (3), 633–646. https://doi.org/10.1016/j.cell.2012.06.029. S0092-8674(12)00786-6 [pii].

Paxinos, G., Watson, C., 1998. The Rat Brain in Stereotaxic Coordinates. Academic Press, San Diego.

Rice, A.C., Floyd, C.L., Lyeth, B.G., Hamm, R.J., DeLorenzo, R.J., 1998. Status epilepticus causes long-term NMDA receptor-dependent behavioral changes and cognitive deficits. Epilepsia 39 (11), 1148–1157.

Sankar, R., Shin, D.H., Liu, H., Mazarati, A., Pereira de Vasconcelos, A., Wasterlain, C.G., 1998. Patterns of status epilepticus-induced neuronal injury during development and long-term consequences. J. Neurosci. 18 (20), 8382–8393.

Sattler, R., Xiong, Z., Lu, W.Y., MacDonald, J.F., Tymianski, M., 2000. Distinct roles of synaptic and extrasynaptic NMDA receptors in excitotoxicity. J. Neurosci. 20 (1), 22–33.

Saur, L., Baptista, P.P., de Senna, P.N., Paim, M.F., do Nascimento, P., Ilha, J., Bagatini, P.B., Achaval, M., Xavier, L.L., 2014. Physical exercise increases GFAP expression and induces morphological changes in hippocampal astrocytes. Brain Struct. Funct. 219 (1), 293–302. https://doi.org/10.1007/s00429-012-0500-8.

Schartz, N.D., Herr, S.A., Madsen, L., Butts, S.J., Torres, C., Mendez, L.B., Brewster, A.L., 2016. Spatiotemporal profile of Map2 and microglial changes in the hippocampal CA1 region following pilocarpine-induced status epilepticus. Sci. Rep. 6, 24988. https://doi.org/10.1038/srep24988. srep24988 [pii].

Schmued, L.C., Stowers, C.C., Scallet, A.C., Xu, L., 2005. Fluoro-Jade C results in ultra high resolution and contrast labeling of degenerating neurons. Brain Res. 1035 (1), 24–31 S0006-8993(04)01849-9 [pii].

Szczurowska, E., Mares, P., 2015. Different action of a specific NR2B/NMDA antagonist Ro 25-6981 on cortical evoked potentials and epileptic afterdischarges in immature rats. Brain Res. Bull. 111, 1–8. https://doi.org/10.1016/j.brainresbull.2014.11.001. S0361-9230(14)00175-0 [pii].

Tavassoli, E., Saboory, E., Teshfam, M., Rasmi, Y., Roshan-Milani, S., Ilkhanizadeh, B., Hesari, A.K., 2013. Effect of prenatal stress on density of NMDA receptors in rat brain. Int. J. Dev. Neurosci. 31 (8), 790–795. https://doi.org/10.1016/j.ijdevneu.2013.09.010. S0736-5748(13)00139-1 [pii].

Trinka, E., Cock, H., Hesdorffer, D., Rossetti, A.O., Scheffer, I.E., Shinnar, S., Shorvon, S., Lowenstein, D.H., 2015. A definition and classification of status epilepticus–report of the ILAE task force on classification of status epilepticus. Epilepsia 56 (10), 1515–1523. https://doi.org/10.1111/epi.13121.

van Esch, A., Ramlal, I.R., van Steensel-Moll, H.A., Steyerberg, E.W., Derksen-Lubsen, G., 1996. Outcome after febrile status epilepticus. Dev. Med. Child Neurol. 38 (1), 19–24.

Vartanian, M.G., Barton, M.E., Boxer, P.A., White, H.S., 2000. The Anticonvulsant Profile of CI-1041, a Novel NR1/NR2B Subtype Selective NMDA Antagonist. Program No. 528.16. Neuroscience Meeting Planner. Society for Neuroscience, New Orleans, LA 2000, Online. Abstr.

Velisek, L., Mikolasova, R., Blankova-Vankova, S., Mares, P., 1989. Effects of ketamine on metrazol-induced seizures during ontogenesis in rats. Pharmacol. Biochem. Behav. 32 (2), 405–410 0091-3057(89)90170-6 [pii].

Veliskova, J., Velisek, L., Mares, P., Rokyta, R., 1990. Ketamine suppresses both bicuculline- and picrotoxin-induced generalized tonic-clonic seizures during ontogenesis. Pharmacol. Biochem. Behav. 37 (4), 667–674.

Vezzani, A., French, J., Bartfai, T., Baram, T.Z., 2011. The role of inflammation in epilepsy. Nat. Rev. Neurol. 7 (1), 31–40. https://doi.org/10.1038/nrneurol.2010.178. nrneurol.2010.178 [pii].

Wang, X.M., Bausch, S.B., 2004. Effects of distinct classes of N-methyl-D-aspartate receptor antagonists on seizures, axonal sprouting and neuronal loss in vitro: suppression by NR2B-selective antagonists. Neuropharmacology 47 (7), 1008–1020 S0028390804002333 [pii].

Wang, L., Liu, Y.H., Huang, Y.G., Chen, L.W., 2008. Time-course of neuronal death in the mouse pilocarpine model of chronic epilepsy using Fluoro-Jade C staining. Brain Res. 1241, 157–167 S0006-8993(08)01831-3 [pii].

Whittemore, E.R., Ilyin, V.I., Woodward, R.M., 2000. Electrophysiological Characterization of CI-1041 on Cloned and Native NMDA Receptors. Program No. 527.3. Neuroscience Meeting Planner. Society for Neuroscience, New Orleans, LA 2000, Online. Abstr.

Wroge, C.M., Hogins, J., Eisenman, L., Mennerick, S., 2012. Synaptic NMDA receptors mediate hypoxic excitotoxic death. J. Neurosci. 32 (19), 6732–6742. https://doi.org/10.1523/JNEUROSCI.6371-11.2012. 32/19/6732 [pii].

Wu, D., Miyamoto, O., Shibuya, S., Okada, M., Igawa, H., Janjua, N.A., Norimatsu, H., Itano, T., 2005. Different expression of macrophages and microglia in rat spinal cord contusion injury model at morphological and regional levels. Acta Med. Okayama 59 (4), 121–127. https://doi.org/10.18926/AMO/31950.

Wyatt-Johnson, S.K., Herr, S.A., Brewster, A.L., 2017. Status epilepticus triggers time-dependent alterations in microglia abundance and morphological phenotypes in the Hippocampus. Front. Neurol. 8, 700. https://doi.org/10.3389/fneur.2017.00700.

Yankam Njiwa, J., Costes, N., Bouillot, C., Bouvard, S., Fieux, S., Becker, G., Levigoureux, E., Kocevar, G., Stamile, C., Langlois, J.B., Bolbos, R., Bonnet, C., Bezin, L., Zimmer, L., Hammers, A., 2016. Quantitative longitudinal imaging of activated microglia as a marker of inflammation in the pilocarpine rat model of epilepsy using [11C]-(R)-PK11195 PET and MRI. J. Cereb. Blood Flow Metab. https://doi.org/10.1177/0271678X16653615. 0271678X16653615 [pii].

Zhou, X., Hollern, D., Liao, J., Andrechek, E., Wang, H., 2013. NMDA receptor-mediated excitotoxicity depends on the coactivation of synaptic and extrasynaptic receptors. Cell Death Dis. 4, e560. https://doi.org/10.1038/cddis.2013.82. cddis201382 [pii].